Layered composites based on niobium with silicide-carbide or silicide-boride hardening

Korzhov Valery Polikarpovich, Kiiko Vyacheslav Mikhailovich, Prokhorov Dmitry Vladimirovich, Zheltyakova Irina Sergeevna
Institute of Solid State Physics, Russian Academy of Sciences, Chernogolovka, Moscow Region

Abstract: *The work is devoted to the development of a solid-phase technology for obtaining high-temperature layered composites from Nb-alloys. The following are presented: one of the options for the formation of the initial multilayer package and its diffusion welding (1), the microstructure of the obtained composites (2) and the results of testing composites (3) for strength at room temperature and temperatures up to 1350°C, taking into account the structure anisotropy, crack resistance and tests for creep with two options for processing the obtained experimental data.*
***KEYWORDS**: COMPOSITE, HEAT RESISTANCE, LAYERED STRUCTURE, NIOBIUM, CREEP, CARBIDE-SILICIDE, CARBIDE-BORIDE, STRENGTH, CRACK RESISTANCE, DIFFUSION WELDING, SOLID PHASE TECHNOLOGY*

1. Introduction

Workings of constructional materials designed for use at high temperatures, based on niobium and molybdenum can result in materials with the highest operating temperature ceiling. The especially high modulus of elasticity for molybdenum and its intermetallic compounds suggests that materials based on it can achieve the highest strength [1–3]. High melting points, strength at high temperatures and creep resistance of niobium and molybdenum compounds, as well as the possibility of organizing increased resistance to oxidation, as, for example, in Mo–Si–B alloys [4], open up a real prospect for obtaining heat-resistant composites based on them.

In addition, the combination of molybdenum or niobium and their purely intermetallic compounds or carbide-silicides in the structure of the composite makes it possible to reduce the density of the composite in comparison with the density of these metals due to the relatively low density of intermetallic compounds and carbide-silicides of niobium and molybdenum [5].

The problem of fracture toughness of composites, which exists in connection with the presence of brittle compounds in their structure, is not insurmountable. One of the possibilities of its solution by decelerating cracks at a weak interface between brittle phases was first shown back in 1964 in [6]. This idea was later used in the development of various layered and fibrous composite materials [7, 8].

In the work, the authors used a "non-melting" method for producing flat products from Nb-alloys, free from the problems of their compatibility with the crucible and guaranteeing the direction of the structure to the product. For its formation, a diffusion method was used, which consists in the solid-phase interaction of two or more components. The directionality of the structure and the interaction of the components were achieved in multilayer stacks of metal foils during their diffusion welding under pressure.

2. Heat-resistant composites from Nb-alloys

2.1. Composites Nb/(Si–C)1 and Nb/(Si–C)2

We investigated layered composites of a multicomponent Nb- alloy with silicide-carbide hardening, obtained by diffusion welding of multilayer packages under pressure in vacuum. The structure of composites was set already at the stage of package assembly.

The elements of the assembly were U-shaped elements made of Nb-foils coated with a multicomponent powder mixture (Fig. 1). The number of items in the package – 15 pcs. Nb foil thickness – 50 microns. One outer and one inner side of the U-elements were coated with a suspension layer of a multicomponent mixture of powders in polyvinyl glycol. Coating composition: 55.2Nb–22.0Ti–8.9Mo–5.6Si–5.4ZrH_2–1.7Cr–1.2 wt. %Al. The zirconium in the powder mixture was in the form of a hydride. Hydrogen was removed from the coating by heating, starting from 350–400°C. The package, made of U-elements, retained its integrity by alternating Nb-foils and coatings. The number of Nb-layers in a package is 30 *pcs.*, The number of coatings is one less.

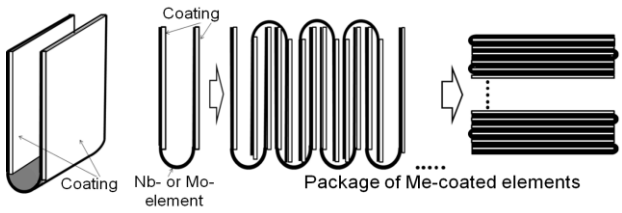

***Fig. 1.** Coated element and multilayer bag assembly diagram. On the right is a package made up of U-shaped elements with one inner and one outer cover.*

Diffusion welding of packages Nb/(Si–C)1 and Nb/(Si–C)2 was carried out at 1400°C, but in two modes that differed in welding time and pressure: 1–5 *h* at 8.4 *MPa* and 2 – 10 hours at 15.3 *MPa*. Carbon penetrated into the powder coating while welding the bags from the atmosphere in the welding chamber with a graphite heater.

In fig. 2 shows the microstructures of layered composites Nb/(Si–C)1 and 2. Their thickness after welding is 3.3 and 2.7 *mm*, respectively. Composite thickness with longer welding times was noticeably thinner. The structures are similar in that they consisted of layers inheriting the Nb-foil and layers of the products of sintering powder coatings and their diffusion interaction with the Nb-foil. In the structures of both composites, the layers are designated as (Nb,Ti), indicating that this is an alloy in which the main elements are niobium and titanium. For example, in the Nb/(Si–C)1 (Nb,Ti)-layers the composition was 66.5Nb–24.3Ti–9.2 at. %Me (Me – Mo, Cr, Al and Si) with "traces" of carbon.

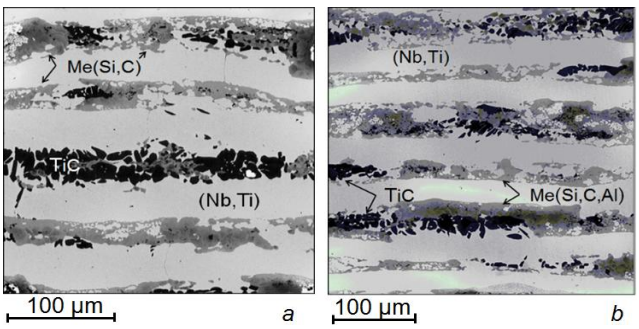

***Fig. 2.** Microstructure of composites Nb/(Si–C)1 and 2 after diffusion welding at 1400°C: a – 5 h and 8.4 MPa; b – 10 h and 15.3 MPa*

In composite 2, a change in the concentrations of phase-forming elements, Nb and Ti, in the carbide-silicide phase was traced with distance from the boundary with the (Nb,Ti)-layer. The composition varied from almost equal concentrations of Ti and Nb, ~23.6 at. %, to a concentration ratio in favor of titanium 34.6 at. %Ti and 13.8 at. %Nb → 42.6 at. %Ti and 3,6 at. %Nb:

$$(Ti_{0.47}Nb_{0.47}Me_{0.17})_{1.11}(Si_{0.60}Al_{0.03}C_{0.26})_{0.89} \rightarrow$$
$$\rightarrow (Ti_{0.69}Nb_{0.28}Me_{0.15})_{1.12}(Si_{0.59}Al_{0.02}C_{0.20})_{0.88} \rightarrow$$
$$\rightarrow (Ti_{0.85}Nb_{0.07}Me_{0.24})_{1.16}(Si_{0.61}Al_{0.05}C_{0.17})_{0.84}.$$

The unidentified phase in the composites was a dark gray phase localized within the Me(Si,C) or Me(Si,C,Al) phases. It is not marked in the figures, but according to local X-ray spectral analysis, it is based on Nb, Si, and C: 53.7Nb–0.5Ti–0.2Cr–30.6Si–15.0 at. %C. In terms of concentration, this phase can be assigned to the eutectic regions: (Nb) + α-$(Nb,Me)_5(Si,C)_3$ of the Nb–Si phase diagram or to (Nb) + β-$(Nb,Me)(C, Si)_2$ of Nb–C phase diagrams.

Mechanical characteristics. After DW, the packages had the form of plates, from which specimens were cut in the form of rectangular rods for strength testing by the 3-point bending method at room temperature and high, up to 1350°C, temperatures.

Crack resistance tests were performed on notched specimens. The critical stress intensity factor *K** was calculated under plane deformation conditions using the formula:

$K^* = [P \cdot S \cdot f(a/W)]/B \cdot W^{3/2}$, where *P* is the maximum load, *S* is the base or distance between the supports, *B* and *W* are the width and height of the specimen, and are the depth of the notch. The load was applied from the side opposite to the notch.

Together with the *K** measurements, the effective surface destruction energy *g* of the sample was determined. In theory, strength testing is considered as the separation of a sample into two parts by a macroscopic crack and the formation of two fracture surfaces. Then *g* can be estimated by the ratio of the work of external forces to the doubled area of its cross-section:

$g = (1/2F) \int Q(x)dx$, where *Q* is the load on the sample, *x* is the deflection and *F* is the cross-sectional area of the sample. In reality, this is the area under the experimental load-deflection relationship.

Since the layered structure of the composite has anisotropy, it was useful to apply the load *P* perpendicularly (⊥) and parallel (||) to the layers (*ab*) in the tests for strength and crack resistance for their assessment. In fig. Fig. 3 shows the dependences of the ultimate strength on the testing temperature of the composites Nb/(Si–C) 1 and 2. It was expected that with a load applied parallel to the layers, the strength would be higher. This was the case for the Nb/(Si–C)2 composite (see symbols ○ in Fig. 3, *b*). This is due to the higher moment of resistance of the carbide-silicide layers with a parallel orientation of the direction of application of the load and the plane of the layers. But for the Nb/(Si–C)1 composite with a shorter welding time and pressure at 20°C, this was not observed (see Fig. 3, *a*). Moreover, for P ‖ (ab) σ_B was even less.

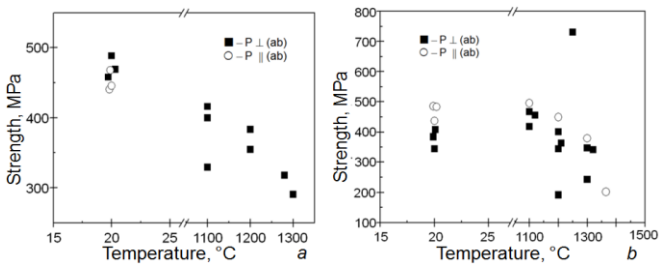

Fig. 3. *Dependences of the ultimate strength σ_B for composites Nb/(Si–C)1 (a) and 2 (b) on the test temperature at P ⊥ (ab) (■) and P ‖ (ab) (○)*

At 20°C, composite 1 had σ_B in the range from 440 to 490 *MPa*, composite 2 – 350–490 *MPa*. However, during temperature tests, the tensile strength of the Nb/(Si–C)1 composite after welding for 5 *h* monotonically decreased, while for the Nb/(Si–C)2 composite after 10 *h* welding σ_B remained at a constant level up to 1200°C. Yes, the strength values had a significant scatter: ~200 *MPa* at 1200°C, but ... there was a measurement at 1250°C with $\sigma_B \approx 750$ *MPa*. According to metallographic analysis data, the crack-resistant structural phase of composite 2 occupied ~66% of the volume. The hardening phases accounted for 15 (carbide) and 16% (intermetallic) volumes. Judging by the experimental data, such a volume of hardening phases is not so small. Probably, the ratio of viscous-plastic and high-strength phases is close to the optimal value, which is reflected in high values of strength at 1100°C and above. For the Nb/(Si–C)1 composite, after diffusion welding for 5 *h*, the crack-resistant component occupied a noticeably larger part of the volume, ~77 vol.%. [The volume amounts of phases were calculated from micrographs (see Fig. 2), in which the TiC, (Nb,Ti) and Me(C,Si)- or Me(C,Si,Al)-phases were colored in different colors].

The results of testing the Nb/(Si–C)2 composite for crack resistance with the calculation of the critical coefficient *K** and the effective surface energy of destruction *g* are summarized in Table. 1. The anisotropy of the structure led to a noticeable difference in the values of fracture toughness *K**, which was 12.8 ± 1.9 when a load was applied perpendicularly and 10.4 ± 1.7 $MPa \cdot m^{1/2}$ – parallel to the layers of the structure.

Table 1. *Results of tests of composites Nb/(Si–C)1 and Nb/(Si–C)2 for crack resistance*

	K*, $МПа \cdot м^{1/2}$	g, $Дж/м^2$		K*, $МПа \cdot м^{1/2}$	g, $Дж/м^2$
P ⊥(ab)	12,0	2690	P ‖(ab)	7,9	2230
	10,8	2120		12,9	2430
	15,6	3280		10,5	1530

The difference in *g* values when a load is applied ⊥-ly and ‖-el to the layers of the structure is explained by the involvement of various types of microfractures in the total fracture and in their number when the macrocrack passes perpendicularly (Fig. 4) or parallel to the layers.

It is of interest to establish a correlation between fracture toughness *K** and effective surface energy *g* (Fig. 5). Based on the still limited data set, it can be stated that the growth of parameters occurs simultaneously.

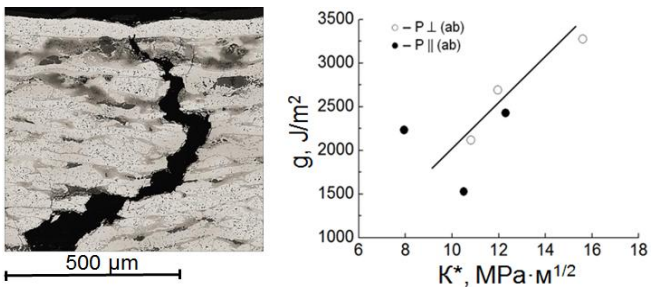

Fig. 4. Trajectory of a macrocrack in the fracture site of the Nb/(Si–C)2 composite at P⊥ (ab)
Fig. 5. Correlation of fracture toughness K with effective surface energy g*

Creep tests. At this stage of the work, for testing samples for creep, the scheme of their 3-point loading was chosen, as one of the most acceptable in terms of requirements for the manufacture of samples (their shape and size). Taking into account the conditions and limitations of this scheme [9], as well as using unconventional methods of processing experimental data [10, 11], it is possible to obtain (as preliminary) results of creep tests for a comparative analysis of the characteristics of developed materials in a relatively short time. Such tests seem to be especially convenient in the conditions of the initial stage of research work.

The high-temperature tests were carried out in the same chamber and according to the scheme as the 3-point bending tests, as well as taking into account the results previously obtained when testing specimens of the same material for short-term strength. The specimen was "stepwise" loaded with specified loads and held at each load under steady-state creep conditions. During the tests, the temperature, load, time and deflection of the sample were recorded. The processing of the results was done proceeding from the power law of creep in tension [12], that is, the behavior of the material in tension was simulated from bending tests: $\dot{\varepsilon} = \eta_n (\sigma/\sigma_n)^n$, where $\dot{\varepsilon}$ is the creep rate, η_n, σ_n and n are constants, one of which must be chosen arbitrarily. Let $\eta_n = 10^{-4}\ h^{-1}$. This means that stress σ_n causes 1% deformation in 100 hours. Following the scheme ([10, 12]) for solving the problem of rod bending under steady-state creep conditions, for our case we obtain an expression that relates the

value of the applied load P [*MPa*] and the deflection rate *v* [*μm/h*] at the center of the rod, i.e. at the place of load application:

(1) $$v = \eta_n \frac{L}{2^{2(n+1)}(n+2)\xi^n(n)} \left(\frac{2P}{\sigma_n bh}\right)^n \left(\frac{2L}{h}\right)^{n+1}$$, where $$\xi(n) = \frac{2n}{2n+1}$$, *L* is the base length, *b* and *h* are the width and height of the sample. Determining the rate of steady-state creep *v* at various loads from the experimental dependences using expression (1), the values of σ_n and *n* were obtained for the tested samples.

In tests for creep (long-term strength), the sample was loaded with a given load according to the 3-point bending scheme and held there for a given time. The movement of punches was recorded depending on the time. First, there was a choice of clearances in the supports and equipment. When this process ended, the movement of the punch reflected only the deflection of the specimen (Fig. 6, linear sections). The loads were 2, 5 and 6 *kg*. At 2 kg, the sample did not bend for more than 13 hours, which corresponded to the horizontal line of the time dependence of the bending.

The processing of the obtained creep data is as follows.

The exponent n in equation (1) for the deflection rate *v* was determined from the expression

$$v_5/v_6 = (P_5/P_6)_n \text{ , as } n = lg_{(P5/P6)}(v_5/v_6),$$

where P_5 and P_6 are known loads 5 and 6 *kg*, respectively, in the 2nd and 3rd experiments of creep tests, and v_5 and v_6 are the deflection rates calculated similarly to the tangents of the inclination angles of the steady-state creep lines in the 2nd and 3rd experiments, respectively. Indexes 5 and 6 at *v* and *P* repeat loads of 5 and 6 *kg*. Next, we obtain the values of σ_n and n for the tested sample at 1100°C: σ_n = 80.0 *MPa* and n = 3.78. And, finally, we construct the dependence of the creep strain rate έ on the stress σ (Fig. 7).

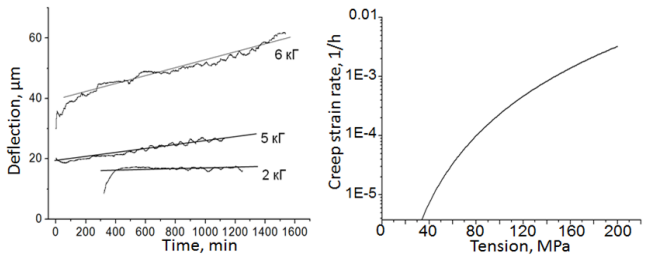

Fig. 6. *Dependence of the deflection in bending on the test time at 1100°C and a load of 2, 5, and 6 kg for the Nb/(Si–C)2 composite*

Fig. 7. *The rate of creep deformation in tension έ depending on the stress σ at v corresponding to 6 kg for the Nb/(S–C)2 composite at 1100°C*

Using the constructed dependence έ = f(σ), we estimate the strength of the obtained composite loaded with a stress of 50 *MPa*. This stress corresponds to the creep strain rate έ, equal to $1.07 \cdot 10^{-5}$ h^{-1}. You can find out how much a rod of length *l* = 100 *mm* will elongate, made of this material in 100 hours: έ = (Δl/l)/ΔT, то

$$\Delta l = \acute{\varepsilon} \cdot \Delta T \cdot l = 1{,}07 \cdot 10^{-5}\ ч^{-1} \cdot 100\ ч \cdot 100\ мм = 0{,}11\ мм.$$

The elongation was 0.11 *mm*.

Conclusions for the section. Microstructure studies show in favor of the chosen method of obtaining heat-resistant composites from multicomponent alloys. Without resorting to melting technologies, layered composites of an alloy of niobium with Ti, Mo, Cr, Zr and Al, strengthened by the compounds of these metals with carbon and silicon, were obtained.

1. The results of strength tests at long exposures and high welding temperatures are aimed at obtaining completed multilayer or layered structures.

2. The values of fracture toughness K* of composites are such that they occupy a position between ceramics and high-strength metal alloys, which is not satisfactory enough. It is possible to improve K* (1) by increasing the proportion of viscous-plastic (Nb)-solid solution in the layered structure of the composite. But it seems more efficient (2) to preserve the viscous-plastic state of the layers inheriting metal alloys in the foil composite.

The point is that Nb foils and alloy foils become stronger as a result of the penetration of carbon, silicon and boron into them during diffusion welding of the packages. To prevent this from happening, it is possible to pre-arrange diffusion barriers against the penetration of C, Si, and B into the visco-plastic layers of the composite, which, possibly, can be thin layers of the same carbides, silicides, and borides.

2.2. Composite Nb/(Si–C)3.

The composite was prepared using a slightly different technique than composites Nb/(Si–C)1 and Nb/(Si–C)2. First, a 2-sided suspension coating of a powder mixture of niobium with Ti, Mo, ZrH_2, Cr, and Al of a certain concentration was applied to the Nb-foils. Coated foils and sections of TRG (thermally expanded graphite) tapes were used to make up a multilayer package, which was heat treated under pressure at a temperature of 1500°C for 2–3 hours. After the package was disassembled (it was easily disassembled), a silicon coating was applied to its surface, and a package was made from such segments, from which, after diffusion welding under pressure, a layered composite in the form of a plate 3–4 mm thick was obtained.

During the second welding, the final sintering (1) of the powder mixture already with silicon and additional penetration of carbon into it, (2) additional alloy formation, (3) diffusion formation of metal carbide-silicides and, in fact, (4) the formation of a layered composite took place. The result of welding in the form of a microstructure of a cross-section at two magnifications and a cross-section of the composite in the fracture zone after a short-term bending test is shown in Fig. 8 and 9.

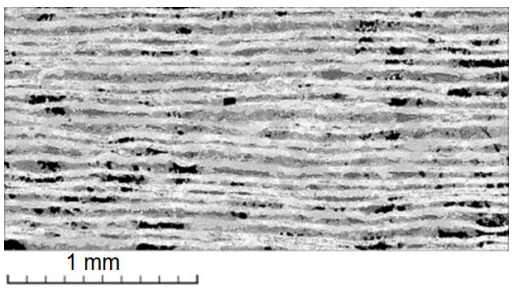

Fig. 8. *Composite Nb/(Si–C)3. Macrostructure of a cross-section after diffusion welding at 1500°C and a pressure of 19 MPa for 3 h*

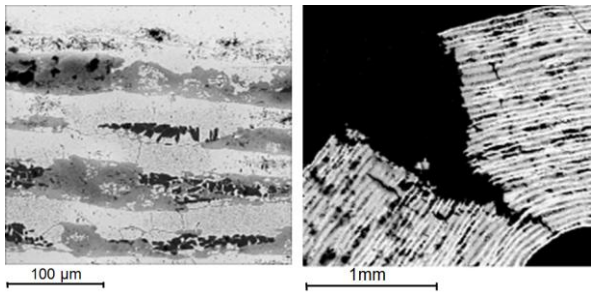

Fig. 9. *Microstructure of the Nb/(Si–C)3 composite after welding and its cross section at the fracture site during 3-point bending tests*

The light layers are identified as Nb-solid solution in place of Nb-foils, between which there are reinforcing layers of metal carbide-silicides.

Creep tests. The composite was subjected to creep tests. The experiments consisted of holding the samples under load at a constant temperature. Temperature range – 1150, 1200, 1250 and 1300°C. The load values were significantly less than the load at which the sample was destroyed during short-term tests. In the experiments, the dependences of the sample deflection on time were obtained. To determine the creep characteristics, the dependence of the creep rate on stress and temperature was used: $\acute{\varepsilon} = K \cdot \sigma_n \cdot e^{Q/kT}$ [equation (1)], where: έ is the creep strain rate, *K* is a constant, *σ* is the stress, *n* is the rate sensitivity index strain to stress, *Q* is the

activation energy, k is the Boltzmann constant, T is the temperature. The starting points for calculating the parameters of Eq. (1) were the time dependences of the deflection value experimentally measured for each sample at the stage of steady-state creep at three applied stresses and two temperatures. From the data obtained, the deflection rate f was determined.

The relative strain rate $\acute{\varepsilon}$ in the section of steady creep was calculated using the formula for the strain rate (in s^{-1}): $\acute{\varepsilon} = 4h \cdot f/l^2$ (2), where f is the deflection rate (*mm*/s), h is the sample height (mm) and l is the distance between the supports (mm). For further calculations, equation (2) was represented as

$$\acute{\varepsilon}_0 = (s_0/\sigma_0)^n \times (\sigma/s_0)^n \times e^{-Q/kT}, \quad (3)$$

where s_0 = 1 MPa, $\acute{\varepsilon}_0$ (s^{-1}) and σ_0 (MPa) are constants. At constant temperature, expression (3) was represented as: $\acute{\varepsilon} = N \times (\sigma/s_0)^n$ (4), where $N = \acute{\varepsilon}_0 \cdot (s_0/\sigma_0)^n \cdot e^{-Q/kT}$ [equation (5)].

The parameters N and n are determined from the graph $\acute{\varepsilon} = f(\sigma)$, presented in logarithmic coordinates, at each test temperature.

The constants $M = \acute{\varepsilon}_0 \times (s_0/\sigma_0)^n$ and Q were determined from two equations (5) for two different temperatures (Fig. 10).

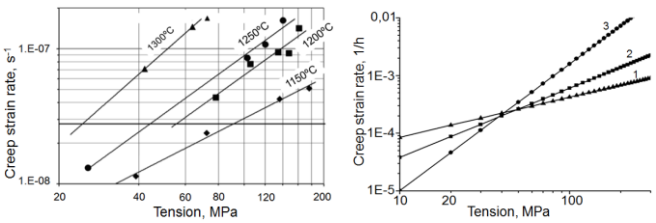

Fig. 10. *Dependences of the creep rate on stress for the Nb/(Si–C)3 composite at temperatures in the range 1150–1300°C.*
Horizontal line drawn at 100-hour strength

Fig. 11. *Dependences of the creep strain rate $\acute{\varepsilon}$ on stress for the composite Nb/(Si–C)3: 1 – 50 MPa, 1150°C; 2 – 52.55 MPa, 1150°C; 3 – 45.28 MPa, 1300°C*

Evaluation of the dependence of the creep strain rate of the composite at different temperatures shows that the 100-hour creep limit (horizontal line in the figure) of the Nb/(Si–C)3 composite decreases with an increase in the test temperature from 90 *MPa* at 1150°C to 25 *MPa* at 1300°C (Fig. 10).

The results obtained were compared with similar results for cast (Nb–Si)-alloys obtained by directional solidification. Such studies with the processing of experimental data using a similar technique were carried out in our laboratory. The comparison showed that the Nb/(Si–C)3 composite had a higher level of 100-hour strength than the (Nb–Si)-alloys with a directed structure at 1150°C: 90 and 60 *MPa*, respectively.

Creep tests, but with processing already according to the method known here, which we used for the Nb/(Si–C)2 composite [10–12]. The method simulates flexural testing as the tensile behavior of a material. Using the constructed dependences for $\acute{\varepsilon} = f(\sigma)$, we now estimate the strength of a composite based on a multicomponent Nb-alloy loaded with a stress of 50 *MPa* (Fig. 11). This stress in these experiments at 1150°C corresponds to the creep strain rate $\acute{\varepsilon}$, equal to $0.98 \cdot 10^{-5}$ h^{-1}. Then a rod with a length of l = 100 *mm*, made of such a material, will lengthen by 98 μm in 100 hours: $\acute{\varepsilon} = (\Delta l/l)/\Delta T$, then

$\Delta l = \acute{\varepsilon} \cdot \Delta T \cdot l = 0.98 \cdot 10^{-5}$ $h^{-1} \cdot 100$ $h \cdot 100$ *mm* = 0.098 *mm*.

Note that, in contrast to Fig. 7, here the dependences $\acute{\varepsilon} = f(\sigma)$ are given in logarithmic scales along both axes.

2.3. Composite Nb/(Si–B)

The anisotropy of the layered structure in the composite caused anisotropy of the strength properties in bending tests if a load was applied perpendicularly and parallel to the plane of the layers. The dependence of strength on the test temperature for this composite is shown in Fig. 12. Anisotropy persists at temperatures of 1100–1300°C.

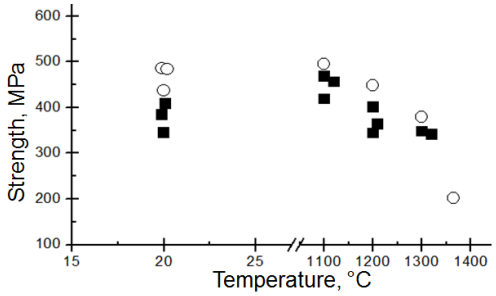

Fig. 12. *Dependence of $\sigma_{B\perp}$ (●) and σ_{B}|| (○) composite Nb/(Si–B) with unpolished surfaces on the test temperature*

The lower strength at room temperature than at 1100°C in the composite was due to the roughness of the two surfaces of the test pieces after spark cutting. For the same composite with surfaces polished after spark cutting, the strengths in the perpendicular and parallel directions at room temperature were equal: $\sigma_{B\perp}$ = (600 ± ± 180) and $\sigma_{B||}$ = (790 ± 48) *MPa*. Anisotropy $\sigma_{B||}/\sigma_{B\perp}$ = 1.32. In high-temperature tests, the quality of the sample surfaces did not affect the strength of the composite. The average strength level of the composite reinforced with silicon and boron compounds was ~450 *MPa* at 1100°C and ~350 *MPa* at 1300°C.

This work was financially supported by the Russian Foundation for Basic Research (project No. 20-03-00296).

REFERENCES

1. Properties, production and application of refractory compounds. Ed. T. Ya. Kosolapov. M.: Metallurgy, 1986, - 928 p.

2. Schneibel J.H. *High temperature strength of Mo–Mo_3Si–Mo_5SiB_2 molybdenum silicides.* Intermetallics, 2003, No 11, pp. 625–632.

3. Sharif A.A., A. Misra, T.E. Mitchell *Strength of $MoSi_2$-based crystals at ultra-high temperature.* Scripta Materialia, 2005, No 52, pp. 399–402.

4. Jain P., K.S. Kumaru *Tensile creep of Mo–Si–B alloys.* Acta Materialia, 2010, v. 58, No 6, pp. 2124–2142.

5. Goronovskii I.T., Yu.P. Nazarenko, E.F. Nekryatch. A short guide to chemistry. Kiev: Naukova dumka, 1987, – 929 c.

6. Cook J., J.E. Gordon. Proceedings of the Royal Society, 1964, v. 282, No 8, pp. 508.

7. Anischenkov V.M., S.T. Mileiko. DAN USSR, 1978, v. 241, No 5, p. 1068.

8. Mileiko S.T. *Oxide-fibre/Ni-based matrix composites – III: A creep model and analysis of experimental data.* Composite Science and Technology, 2001, v. 61, pp.1649–1652.

9. Ruditsin M.N., P.Ya. Artemov, M.I. Lyuboshits. Reference book on the strength of materials. Minsk: Higher school, 1970. – 628 c.

10. *Mileiko S.T. Oxide-fibre/Ni-based matrix composites – III: a creep model and analysis of experimental data*. Composites Science and Technology, 2002, v. 62, pp. 195–204.

11. *Mileiko S.T., V.M. Kiiko. High-temperature creep of fiber composites with a metal matrix at alternating stresses.* Mechanics of Composite Materials, 2004, v. 40, p. 523–534.

12. Ju. N. Rabotnov. Mechanics of a deformable solid. Moscow: Nauka, 1979. –744 p.

13. Karpov M.I., V.I. Vnukov, T.S. Stroganjva et al. Influence of silicon content on microstructure and mechanical properties of an alloy based on the niobium-silicon system. Izvestia RAN. Physical series. 2019, v. 83, No 10, p. 1353–1361.

14. Svetlov I.S., M.I. Karpov, T.S. Stroganjva, D.V. Zaitsev, Yu.V. Artemenko. High-temperature in-situ creep of composites of the Nb-Si system. Deformation and destruction of materials, 2019, No 11, p. 2–6.